


Spectral switches of light in curved space

Suting Ju,¹ Chenni Xu,^{1,2} and Li-Gang Wang ^{1,*}

¹*Zhejiang Key Laboratory of Micro-nano Quantum Chips and Quantum Control, School of Physics, Zhejiang University, Hangzhou 310058, Zhejiang, China*

²*Department of Physics, The Jack and Pearl Resnick Institute for Advanced Technology, Bar-Ilan University, Ramat-Gan 5290002, Israel*



(Received 12 December 2023; accepted 15 May 2024; published 7 June 2024)

Acting as analog models of curved spacetime, surfaces of revolution employed for exploring novel optical effects are followed with great interest nowadays to enhance our comprehension of the universe. It is of general interest to understand the spectral effect of light propagating a long distance in the universe. Here we address the issue of how curved space affects the phenomenon of spectral switches, a spectral sudden change during propagation caused by the finite size of a light source. Based on the point spread function of curved space under the paraxial approximation, the expression of the on-axis output spectrum is derived and calculated numerically. A theoretical way to find on-axis spectral switches is also derived, which interprets the effect of spatial curvature of surfaces on spectral switches as a modification of the effective Fresnel number. We find that the spectral switches on surfaces with positive Gaussian curvature are closer to the source compared with the flat surface case, while the effect is opposite on surfaces with negative Gaussian curvature. We also find that the spectral switches farther away from the light source are more sensitive to the change in Gaussian curvature. This work deepens our understanding of the properties of fully and partially coherent lights propagating on two-dimensional curved space.

DOI: [10.1103/PhysRevA.109.063509](https://doi.org/10.1103/PhysRevA.109.063509)

I. INTRODUCTION

Phenomena in curved spacetime and the physics behind them have been fascinating people since Einstein proposed general relativity. For example, black holes and their event horizons around them, gravity waves, and the universe itself all are still mysterious. In most cases, only passive observation is possible as celestial bodies are far away and their gravitational effect is weak. Fortunately, the idea of analogy provides a new method for us to research them. Nowadays, a variety of analog models have been developed to investigate effects in curved spacetime, such as the water tank [1,2], the Bose-Einstein-condensate system [3,4], light pulses in nonlinear fiber optics [5], and quantum fluids of light [6,7] (see also the reviews in [8–10]).

In condensed-matter physics, the theory of quantum particles confined in curved space was put forth and the geometric potential was discussed [11]. Since the paraxial Helmholtz equation of light on a surface is very similar to Schrödinger's equation, light and plasmonic beams are used to study the propagation mechanism of quantum particles and quantum effects [12–16]. Batz and Peschel considered optical effects in curved space and regarded it as an analog model of general relativity [17]. In this analog model, the curved spacetime is reduced in dimensions and then turned into a two-dimensional surface in this case. Such models can visually

display the geometry of curved space and probably provide new ideas for manufacturing optical devices. There has been interesting research on general relativistic phenomena and optical phenomena in curved space [17–25]. Among them, surfaces with constant Gaussian curvature can act as analog models of universes with nonvanishing cosmological constants and are thus of particular interest in various works [18–22]. For example, Gaussian beams can self-focus on this type of surface with positive Gaussian curvature [18]. It has been theoretically and experimentally found that light does not always gain coherence on this kind of surface, as stated in the Hanbury Brown–Twiss effect [19]. The spectral shift caused by the correlation of a light source has been found to be enhanced by positive curvature and suppressed by negative curvature [20]. The shape-preserving accelerating beams have been theoretically and experimentally realized on the sphere [21]. Recently, the branched flows of light were also interestingly observed on a semispherical bubble [22]. Besides the surfaces of constant Gaussian curvature, Flamm's paraboloid has also been adopted because it is derived from the Schwarzschild metric. Two Flamm's paraboloids can be joined together and form an analog model of wormholes. The effect of tunneling was found when wave packets propagate in this model [23]. There are also some theoretical works considering the propagation of light on more general surfaces of revolution [24–26].

Here we consider the effect of spectral switches of light, a kind of spectral sudden change, on surfaces of revolution. Spectral change of light has attracted a great deal of attention because it can offer or influence the information we get from the spectrum. For example, the Doppler effect can tell us the

*lgwang@zju.edu.cn

relative velocity between a source and an observer. Its further work is the angular Doppler effect. It has applications in rotational Raman scattering, fluorescence doublets, and so on [27]. The theory was also developed to detect spinning objects in astronomy [28]. The spectral change of light may also occur in the propagation of incoherent or correlated light fields in free space [29,30], and this effect is sometimes referred to as the Wolf effect [31,32]. This effect has been experimentally confirmed in different systems [33,34], such as partially coherent light sources [33] and an acoustic experiment [34]. An application of the Wolf effect is spatial-coherence spectral filters, which can be applied in separation of neighboring spectral lines, processing optical signals, and optical coding [35,36].

Exploration of the spectral shift induced by a confined aperture in the near zone led to the revelation of the spectral switch, as initially proposed in [37]. The spectral switch was found to be closely related to spectral anomalies [38]. The definition of the spectral switch is the rapid spectral change between a redshift and a blueshift in certain specific regions. At those positions at which the spectral switch occurs, the spectrum changes drastically and possesses two peaks with the same height. This effect could be induced by the diffraction of fully coherent sources or partially coherent sources obeying the scaling law [38]. For partially coherent sources violating the scaling law, the spectral switch is both diffraction induced and correlation induced [39]. The spectral switch has been experimentally observed [40–43], including circular and rectangular apertures [40], far-field off-axis spectral switches [41], the $1 \times N$ spectral switch [42], and spectral switches in Young's double-slit experiment [43]. There is also research on spectral switches of scattering spectra [44–46]. The effect of spectral switches has important application in lattice spectroscopy [47], spatial-coherence spectroscopy [31], and digital data transmission [48,49]. Although so many studies have been done, optical systems in flat space were the focus of all the previous research. In this work we explore whether spectral switches can happen on two-dimensional curved space and the way the spatial curvature influences the positions of spectral switches.

II. OUTPUT SPECTRUM OF A FINITE LIGHT SOURCE IN CURVED SPACE

A. Point spread function in curved space

A surface of revolution is produced by the rotation of a curve about a certain axis; the curve is called the generatrix. Each point on this surface can be expressed as $\vec{s} = (r(z) \cos \varphi, r(z) \sin \varphi, h(z))$, where $r(z)$ is the expression of the generatrix which satisfies $(dr/dz)^2 + (dh/dz)^2 = 1$. The parameter z represents the proper length along the generatrix and φ represents the rotation angle. The Gaussian (intrinsic) curvature $K = 1/R_1 R_2$ and the extrinsic (mean) curvature $H = (1/R_1 + 1/R_2)/2$ are often used to describe the characteristics of a surface, where R_1 and R_2 represent the radii of the maximal and minimal circles, respectively, that are tangent to the surface at the same point. If these two circles are on the opposite sides of the surface, the Gaussian curvature K will be negative. When the surface has a constant Gaussian curvature,

its generatrix is

$$r(z) = r_0 \cos_q(z/R) = \begin{cases} r_0 \cos(z/R), & q = 1 \\ r_0 \cosh(z/R), & q = -1, \end{cases} \quad (1)$$

where $q = \text{sgn}(K)$ and r_0 is the radius of the equator. The parameter R is the radius of the surface's curvature and then its Gaussian curvature is $|K| = 1/R^2$. In the situation of $K > 0$, the relative difference between R and r_0 can influence the shape of the surface. For $R > r_0$, it is a spindle with $|z| < \pi R/2$; for $R = r_0$, it becomes a sphere with the same range value for z ; and for $R < r_0$, it changes into a bulge with $|z| < R \sin^{-1}(R/r_0)$. When $K < 0$, the shape of the surface is always hyperboloid with $|z| < R \sinh^{-1}(R/r_0)$. The shape of the surfaces with different R and r_0 are shown in Fig. 1.

On a general surface of revolution, the light propagation can be described by the scalar Helmholtz equation [17]

$$(\Delta_g + k^2)\Psi = -(H^2 - K)\Psi, \quad (2)$$

where Ψ is the light field, $\Delta_g = \frac{1}{\sqrt{g}} \partial_i (\sqrt{g} g^{ij} \partial_j)$ is the covariant Laplace operator on a surface with the two surface coordinate parameters x^i and x^j , g^{ij} is the inverse form of the metric of the surface g_{ij} , g is the determinant of metric $\det(g_{ij})$, $k = \omega/c$ is the wave number, and c is the speed of light in vacuum. With z for the proper length in the longitudinal direction and $\xi = r_0 \varphi$ for the arc length on the equator, the metric of a general surface of revolution can be written as

$$ds^2 = dz^2 + \left(\frac{r(z)}{r_0}\right)^2 d\xi^2. \quad (3)$$

Substituting Eq. (3) into Eq. (2) and assuming $\Psi = \frac{A}{\sqrt{r(z)}} v(z, \xi) e^{ikz} e^{i\phi}$, under the paraxial approximation, one can obtain

$$2ik \frac{\partial v}{\partial \Xi} + \frac{\partial^2 v}{\partial \xi^2} = 0, \quad (4)$$

where $\Xi(z) = \int_0^z \left(\frac{r_0}{r(z')}\right)^2 dz'$ is the effective propagation distance elaborated in [24] and $\phi = \frac{1}{2k} \int_0^z V_{\text{eff}}(z') dz'$ is the additional phase caused by curved surfaces with $V_{\text{eff}}(z) = \frac{1}{4} \left(\frac{r'(z)}{r(z)}\right)^2 - \frac{1}{2} \frac{r''(z)}{r(z)}$. Equation (4) has a similar form to the Schrödinger equation. On the right-hand side of Eq. (2), the extrinsic curvature H and the intrinsic curvature K are neglected since the radius of surface R we consider here is much larger than the wavelength. For example, the corresponding values of K and H^2 in table experiments are usually the order of $10^0 - 10^2 \text{ m}^{-2}$, while k^2 is roughly 10^{14} m^{-2} . By solving Eq. (4), one obtains the point spread function of light that spreads along $\xi = \text{const}$ (the line of longitude) on the surface, which is [24]

$$h_q(\eta, \xi, z) = \sqrt{\frac{kr_0}{2\pi i \Xi r(z)}} e^{(ik/2\Xi)(\eta - \xi)^2} e^{ikz} e^{i\phi}, \quad (5)$$

where η is the abscissa on the line of nonequator latitude.

B. On-axis spectrum of light in curved space

In order to consider a finite light source, here we assume that the size of the source is $2a$, which can also be seen as a beam of polychromatic partially coherent light passing

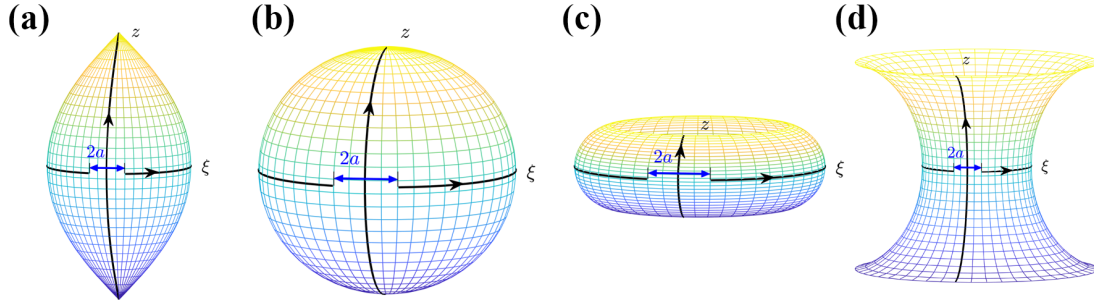


FIG. 1. Different types of surfaces with constant Gaussian curvature and the curvilinear coordinates thereon: (a)–(c) surfaces with constant positive Gaussian curvature and (d) a surface with constant negative Gaussian curvature. The z and ξ are two parameters of surfaces. The slit is settled on $(0,0)$ and its size is $2a$. Light propagates from the slit in the direction of z . When K is positive, the relative size between R and r_0 can influence the shape of the surface, such as (a) a spindle with $R > r_0$, (b) a sphere with $R = r_0$, and (c) a bulge with $R < r_0$. Also shown is (d) the shape of a hyperboloid no matter how we choose R and r_0 .

through a slit with a width of $2a$, as shown in Fig. 1. The light propagates in the direction of $z > 0$, i.e., the line of longitude on the surfaces of revolution. The center of the slit is located at the origin of the coordinate ($z = 0, \xi = 0$). Our aim is to study the spectral change along the propagation, so we first need to obtain the on-axis output spectrum.

The cross-spectral density of a polychromatic partially coherent plane light at the initial place can be expressed as [37]

$$W_{\text{in}}(\xi_1, \xi_2, z = 0, \omega) = S_0(\omega)e^{-(\xi_2 - \xi_1)^2/2\sigma(\omega)^2}, \quad (6)$$

where $S_0(\omega)$ is the initial spectrum and $\sigma(\omega)$ is the rms correlation width. Without loss of generality, we assume that the source satisfies the scaling law and let $\sigma(\omega) = \sigma_0 \frac{\omega_0}{\omega}$. The parameters ξ_1 and ξ_2 represent different points on the initial plane of the light source. We also assume that the spectrum of the source is a Lorentz type with ω_0 the center (or peak) frequency and Γ the half-width of the spectral line, which is expressed as

$$S_0(\omega) = \frac{\Gamma^2}{(\omega - \omega_0)^2 + \Gamma^2}. \quad (7)$$

According to the theory of partially coherent light [50], the cross-spectral density of the light field at the output plane $z > 0$ can be written as

$$W_{\text{out}}(\eta_1, \eta_2, z, \omega) = \int_{-a}^a \int_{-a}^a W_{\text{in}}(\xi_1, \xi_2, z = 0, \omega) \times h_q(\eta_1, \xi_1, z) h_q^*(\eta_2, \xi_2, z) d\xi_1 d\xi_2, \quad (8)$$

where (η_1, z) and (η_2, z) are the different points on the output end, h_q is the point spread function introduced above, and h_q^* is the conjugate function of h_q .

Now we concentrate on the evolution of the light spectrum along the propagation axis, i.e., the line of the longitude by choosing $\eta_1 = \eta_2 = 0$, to achieve the on-axis output spectrum, which can be expressed as

$$\begin{aligned} S(z, \omega) &= W_{\text{out}}(0, 0, z, \omega) \\ &= \frac{\omega a^2 S_0(\omega) r_0}{c\pi \Xi r(z)} \int_0^1 \int_0^1 e^{-a^2(u_1 - u_2)^2/2\sigma(\omega)^2} \\ &\quad \times e^{i(\omega a^2/2c\Xi)(u_1^2 - u_2^2)} du_1 du_2. \end{aligned} \quad (9)$$

In the case of fully coherent light, that is to say, when $\sigma_0 \rightarrow \infty$, the output spectrum becomes

$$S(z, \omega) = \frac{r_0}{r(z)} S_0(\omega) [C(t_{\Xi})^2 + S(t_{\Xi})^2], \quad (10)$$

where $C(x) = \int_0^x \cos(\pi u^2/2) du$ is the cosine Fresnel integral, $S(x) = \int_0^x \sin(\pi u^2/2) du$ is the sine Fresnel integral, and $t_{\Xi} = \sqrt{\frac{\omega a^2}{c\pi \Xi}}$. Note that Ξ is a function of z . For the sake of simplicity, we define $z_0 = a^2/\lambda_0 = \omega_0 a^2/2\pi c$ [37] and use z/z_0 to describe the propagation distance on axis. The Fresnel number at z_0 is 1, so $z/z_0 \ll 1$ means the near-field region and $z/z_0 \gg 1$ means the far-field region.

III. RESULTS AND DISCUSSION

We know that when the weight of the spectral intensity distribution changes, the observed color of light also changes simultaneously. In many situations, the positions of the maximal intensities in spectral curves can usually indicate the important information of the light sources or the light from optical systems. In this context, as the peak frequency in the spectrum shifts towards lower frequencies, the entire spectral profile exhibits a redshift; conversely, as it shifts towards higher frequencies, a blueshift is observed. For the discussion of the redshift or blueshift of a spectral line, here we define a relative spectral shift, without considering the actual shape change of the spectral profile, that is, the relative difference between the peak frequency of the output spectrum at a certain position and the peak frequency of the initial spectrum, which can be expressed as

$$\alpha = \frac{\omega_1 - \omega_0}{\omega_0}, \quad (11)$$

where ω_1 is the corresponding peak frequency of the output spectrum at the observation position. Obviously, under this definition of Eq. (11), when $\alpha > 0$, it is a blueshift, while for $\alpha < 0$, it becomes a redshift. In the following, all our discussion of the redshift or blueshift is based on this definition. From Eq. (9) one can find every ω_1 numerically from the on-axis output spectral information. When there are discontinuity points in the change curve of ω_1 vs the propagation distance z , we call such an effect spectral switches.

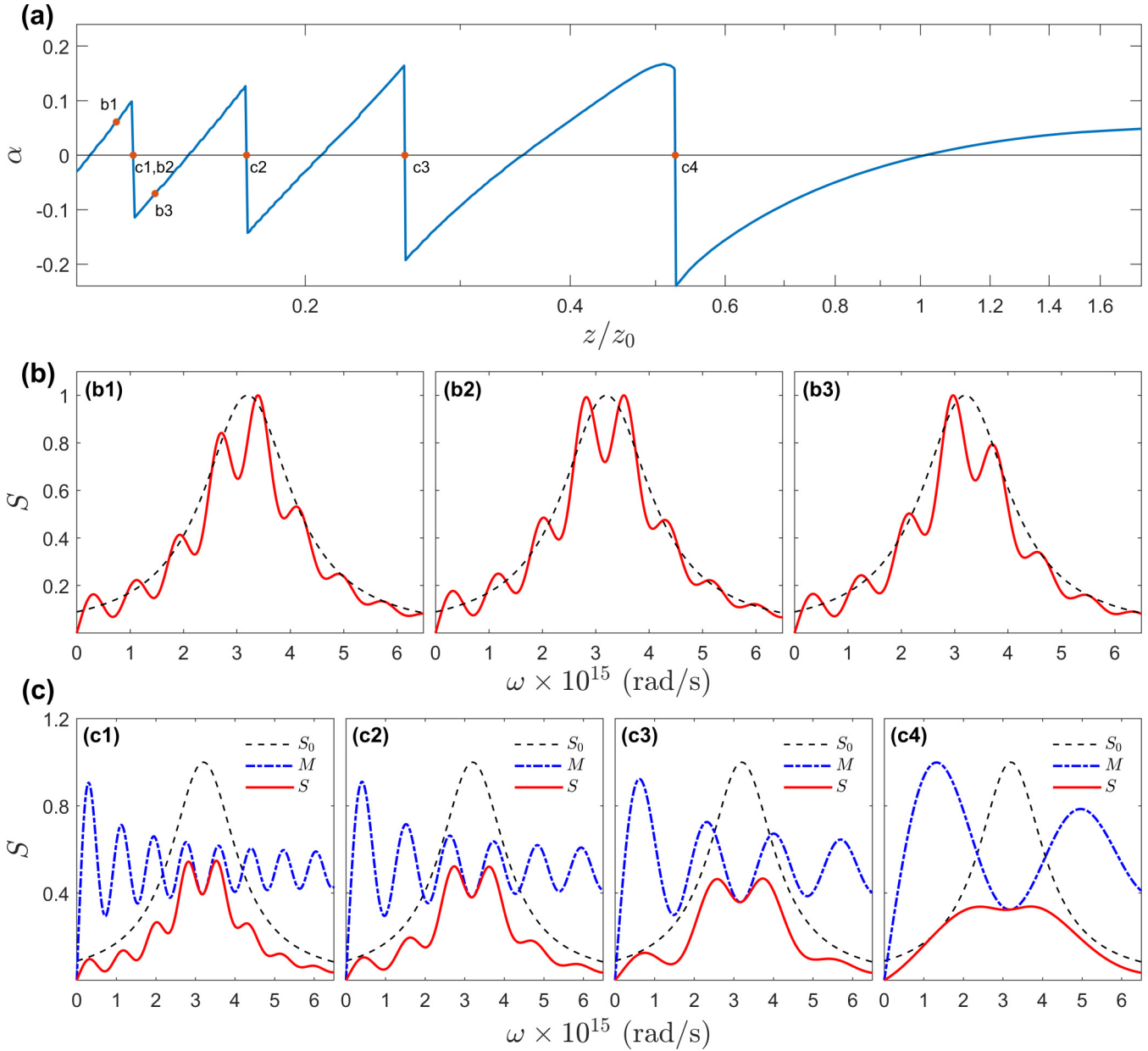


FIG. 2. Effect of spectral switches of a fully coherent light source on the surface with the constant Gaussian curvature $K = 4 \text{ m}^{-2}$. (a) Relative spectral shift curve along the propagation axis. The discontinuity points occur at $z/z_0 = 0.1275, 0.1715, 0.2595, 0.5265$, standing for the positions of spectral switches. (b) Normalized spectral distributions of light at different on-axis positions (b1) $z/z_0 = 0.1220$, (b2) $z/z_0 = 0.1275$, and (b3) $z/z_0 = 0.1350$ near one of the spectral switches ($z/z_0 = 0.1275$). (c) Spectrum profiles at different locations of occurring spectral switches (c1) $z/z_0 = 0.1275$, (c2) $z/z_0 = 0.1715$, (c3) $z/z_0 = 0.2595$, and (c4) $z/z_0 = 0.5265$, corresponding to the fourth, third, second, and first spectral switches, respectively, caused by different valleys of the modifier. Note that in (c1)–(c4), the black dashed curves are the initial spectra, the red solid curves are the output spectra, and the blue dash-dotted curves denote the modifiers at different propagation distances. Here the size of the slit is $2a = 1.0 \text{ mm}$ and the parameters of the initial spectrum [black dashed lines in (b) and (c)] are the center frequency $\omega_0 = 3.2 \times 10^{15} \text{ rad/s}$ and the half-width $\Gamma = 1 \times 10^{15} \text{ rad/s}$.

Figure 2 shows the effect of spectral switches on a surface with positive constant Gaussian curvature. In Fig. 2(a) we observe the change of the relative spectral shift α along the propagation axis. It can be seen that the relative spectral shift α increases from the redshift to the blueshift repeatedly as the propagation distance increases and it suffers sudden drops from the blueshift to the redshift at certain positions (denoted by the points c_1, c_2, c_3 , and c_4) where spectral

switches happen. Figure 2(b) shows the changes of spectral distributions near one of spectral switches, and the ripples of spectral distributions originate from the diffraction of light by the slit. Due to the diffraction of light, the maximal spectral intensity gradually shifts and redistributes with the increase of propagation distance z , and at specific positions there are two maximal (equal) spectral intensities indicating the occurrence of the spectral switch. Accordingly, the relative spectral

shift α changes drastically from positive to negative. Spectral switches occur on these critical points and their spectra are shown in Fig. 2(c).

Here we work out a theoretical method to search for these critical positions of spectral switches, which can help us understand this effect on curved surfaces. The output on-axis spectrum can be rewritten as

$$S(z, \omega) = S_0(\omega)M(z, \omega), \quad (12)$$

where the function $M(z, \omega)$ is usually recognized as the modifier (or the transfer function). We need to find positions where the output spectrum has two peaks with equal heights and a valley between them, so we can turn to search for the valleys of the modifier $M(z, \omega)$. From Fig. 2(c) we find that the modifier has many peaks and valleys and different spectral switches occur when different valleys of the modifier correspond to the central frequency ω_0 . To facilitate further discussion, we classify the spectral switches based on the order of the valley that directly causes the spectral switch. According to the classification, the four spectral switches shown in Fig. 2(c) are, from left to right, the fourth spectral switch, the third spectral switch, the second spectral switch, and the first spectral switch, that is, spectral switches with larger orders are closer to the source. Actually, there are more spectral switches closer to the source, but we only show the four farthest spectral switches in Fig. 2(c) for simplicity.

When the source is fully coherent with $\sigma_0/a \rightarrow \infty$, the modifier can be written as $M(z, \omega) = r_0/r(z)[C(t_\Xi)^2 + S(t_\Xi)^2]$ according to Eq. (10), where $t_\Xi = \sqrt{\omega a^2/\pi c \Xi}$ can be considered as a function of ω in this case and the modifier $M(z, \omega)$ can be seen as $M(z, t_\Xi(\omega))$. By taking the derivative of the modifier to get the equation of the extreme point, we have

$$\frac{\partial M}{\partial \omega} = \frac{\partial M}{\partial t_\Xi} \frac{\partial t_\Xi}{\partial \omega} = \frac{\partial M}{\partial t_\Xi} \sqrt{\frac{a^2}{4\pi c \omega \Xi}} = 0. \quad (13)$$

Since there is always $\sqrt{a^2/4\pi c \omega \Xi} > 0$, our aim is then turned to search for the zero points that satisfy $\partial M/\partial t_\Xi = 0$, i.e., find the local minimum values in $M(z, t_\Xi)$. The expression is

$$C'(t_\Xi)C(t_\Xi) + S'(t_\Xi)S(t_\Xi) = 0. \quad (14)$$

The zero points in Eq. (14) can be obtained numerically and we denote the value of the independent variable of these zero points by v_i ($i = 0, 1, 2, 3, \dots$). The local minimum points occur where i is an even positive integer. Therefore, the condition for the m th local minimum of the modifier $M(z, \omega)$ to occur is $t_\Xi = v_{2m}$ ($m = 1, 2, 3, \dots$). When the m th local minimum point of the modifier coincides with the central frequency ω_0 , the on-axis output spectrum will be very close to the spectral switch, so the approximation expression of the m th on-axis spectral switch is

$$\Xi_m = \frac{\omega_0 a^2}{\pi c v_{2m}^2}, \quad (15)$$

with $m = 1, 2, 3, \dots$. We can understand Eq. (15) in another way, that is, when the effective propagation distance Ξ reaches some specific values, the spectral switches will occur. For example, the expression of effective propagation distance on surfaces with constant Gaussian curvature is

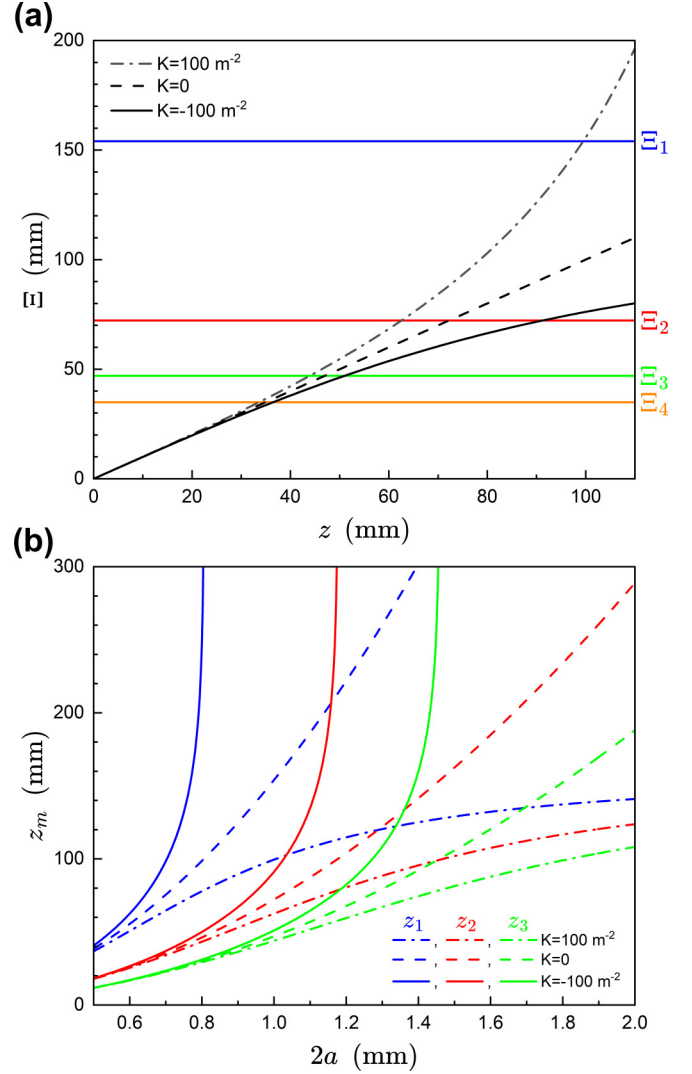


FIG. 3. (a) Effective propagation distance Ξ as a function of z on different surfaces. Different horizontal lines denote the values of the effective propagation distance Ξ_m satisfied for different orders m of spectral switches, i.e., Eq. (15). Here $2a = 1$ mm. (b) Effect of the slit size $2a$ on the positions z_m of the first, second, and third spectral switches on curved surfaces. In (a) and (b) surfaces with curvatures of $K = 100 \text{ m}^{-2}$, $K = 0$, and $K = -100 \text{ m}^{-2}$ are expressed as dash-dotted, dashed, and solid lines, respectively, and the first, second, third, and fourth spectral switches are blue, red, green, and orange, respectively. The source is fully coherent with $\omega_0 = 3.2 \times 10^{15}$ rad/s.

$\Xi = R \tan(z/R)$ for positive curvature and $\Xi = R \tanh(z/R)$ for negative curvature. The on-axis positions for generating the first ($m = 1$, $v_2 = 2.3473$), second ($m = 2$, $v_4 = 3.4284$), third ($m = 3$, $v_6 = 4.2492$), and fourth ($m = 4$, $v_8 = 4.9299$) spectral switches at the fixed effective propagation distances are depicted in Fig. 3(a). The intersection points where the different horizontal colored lines cross the black solid, dashed, and dash-dotted curves of effective propagation distances represent the solutions to the theoretical approximation of spectral switches. Spectral switches on surfaces with positive curvature are closer to the source, whereas they are farther from the source on surfaces with negative curvature.

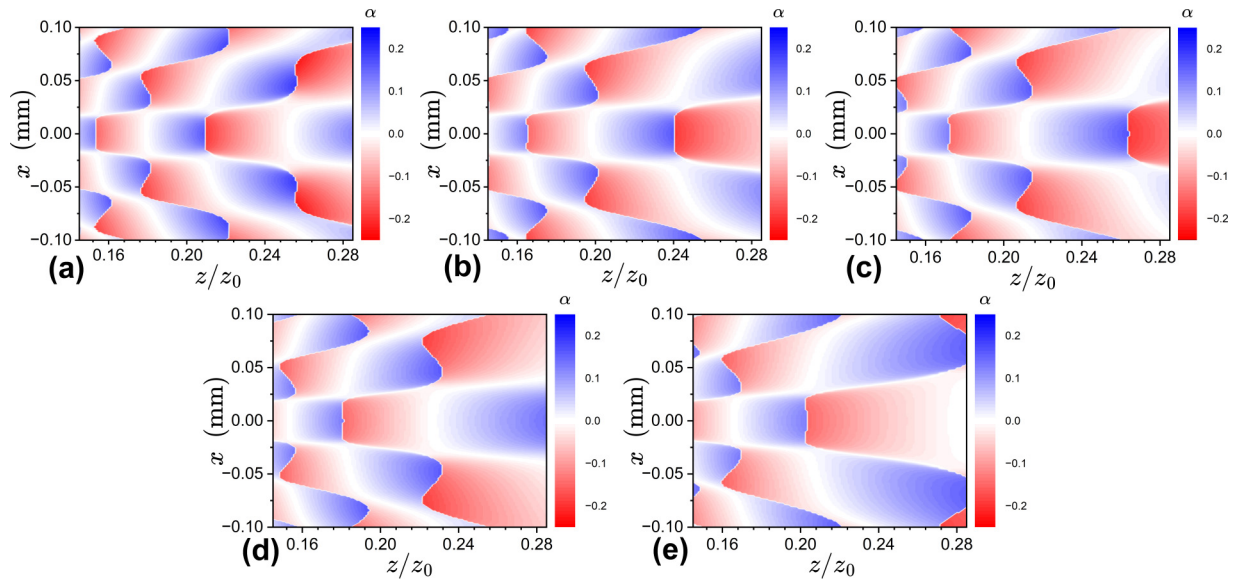


FIG. 4. Distributions of the relative spectral shift α on the different surfaces with various spatial curvatures. The value of Gaussian curvature K is (a) 75, (b) 25, (c) 0, (d) -25 , and (e) -75 m^{-2} . Here the proper length (a) and (b) $x = \eta \cos(z/R)$ and (d) and (e) $x = \eta \cosh(z/R)$. The other parameters are the same as those in Fig. 2.

In Fig. 3(b) we investigate the effect of the slit size $2a$ on the spectral switches, by transforming Eq. (15) into $z_m(a) = R \tan_q^{-1}(\omega_0 a^2 / R \pi c v_{2m}^2)$. As the slit size $2a$ increases, all the positions z_m for the different spectral switches occurring move away from the source. On the surface of negative curvature, since the effective propagation distance increases much more slowly as the value of z increases, the positions z_m for the emergence of the spectral switches increase dramatically as the slit size becomes large. Solid curves in Fig. 3(b) show that the first spectral switch disappears as the value of $2a$ reaches around 0.8056 mm, the second spectral switch exists until $2a$ is close to 1.1768 mm, and the third spectral switch disappears when $2a$ is near 1.4584 mm. On the flat surface of null curvature, the positions z_m for these spectral switches obey the quadratic functions of $2a$. Contrarily, on the surface of positive curvature, since the effective propagation distance Ξ increases rapidly with the increase of z , these values of z_m instead increase much more slowly than the corresponding cases on flat surface as the slit size increases. Such interesting phenomena further reveal the distinct impact of different spatial curvatures on the spectral switches.

In Fig. 4 we demonstrate how the changes of spectral switches evolve from the on-axis situations into the near-axis cases. Here the abscissa η is transformed into the proper length $x = \eta \cos(z/R)$ for $K > 0$ and $x = \eta \cosh(z/R)$ for $K < 0$ in Fig. 4. We choose the vicinity of two spectral switches ($z/z_0 = 0.1727$ and 0.2641) on the flat surface for comparison, as shown in Fig. 4(c). In the case of the positive curvature [Figs. 4(a) and 4(b)], these two spectral switches are both closer to the source. In the case of the negative curvature [Figs. 4(d) and 4(e)], the farther spectral switch is stretched out of the area and the higher-order spectral switches also move away from the source. In Fig. 4 we can see that both the on-axis and off-axis spectral switches are all compressed or stretched due to the increase of the spatial curvature. Although the actual positions for these on-axis and off-axis spectral

switches are different, the rules for the on-axis and near-axis cases are the same. Thus we focus further on the on-axis spectral switches in the following discussion.

Inspired by the previous work [38], spectral switches in three-dimensional (3D) flat space occur when the Fresnel number at the center frequency is an even integer, that is, $N(\omega_0) = 2m$ ($m = 1, 2, 3, \dots$). If we define the effective Fresnel number $N_{\text{eff}} = \omega a^2 / 2\pi c \Xi$ on surfaces of revolution, the quantity $t_{\Xi}(\omega_0)$ can be expressed as $t_{\Xi} = \sqrt{2N_{\text{eff}}}$. Analogously, spectral switches on 2D surfaces of revolution occur when the effective Fresnel number at the center frequency satisfies $N_{\text{eff}}(\omega_0) = z_0 / \Xi = v_{2m}^2 / 2$ ($m = 1, 2, 3, \dots$). Hence, spectral switches for a fully coherent source are also diffraction induced. The difference comes from the infinitesimal dr in 2D space and $rdrd\theta$ in 3D space. In 2D curved space, another notable distinction arises from the nonuniform values of local maxima in the modifier. Consequently, the assigned position corresponds not to the precise spectral switch point but rather to a redshift point slightly preceding it. In contrast, within 3D flat space, the derived expression enables the determination of the exact spectral switch points. The specific form of the modifier in 3D flat space can be found in Ref. [38].

TABLE I. Comparison between the positions of on-axis spectral switches obtained from Eq. (15) and the exact numerical method. The four on-axis spectral switches are chosen in the surface of revolution with the Gaussian curvature $K = 4 \text{ m}^{-2}$ and the light source is fully coherent.

Method/Order	First	Second	Third	Fourth
Eq. (15) (z/z_0)	0.5310	0.2628	0.1727	0.1287
numerical method (z/z_0)	0.5265	0.2595	0.1715	0.1275
relative error	0.75%	1.07%	0.99%	0.54%

Table I presents a comparison of the predicted positions of on-axis spectral switches between the exact numerical method and the theoretical Eq. (15). We use the numerical method to estimate the effectiveness of Eq. (15). As is shown in Table I, we choose four different spectral switches, calculate their positions in both ways, and compare the results. The spectral-switch positions given by Eq. (15) are all slightly larger than their exact positions obtained by the numerical method. The decrease in the values of the local maxima of the modifier with increasing frequency, as illustrated in Fig. 2(c), results in a subtle advanced shift in the positions where spectral switches occur. However, the relative errors are all under 2%, which shows that Eq. (15) works for the cases of fully coherent light. Hence, it is affirmed that Eq. (15) can be initially employed to approximate the positions, followed by a numerical method to precisely determine the locations of spectral switches. It is worth noting that the theoretical method introduced above does not include the influence of r_0 , which is eliminated in the expression of effective propagation distance Ξ . However, the value of r_0 can influence the range of z of the curved surface based on Eq. (1), potentially resulting in the absence of certain spectral switches due to being out of range.

Now let us discuss how the curvatures of surfaces and the spatial correlation of the light source influence the behaviors of on-axis spectral switches. Figure 5(a) displays that the curvatures of curved surfaces do not impact the redshift or blueshift values on either side of the discontinuity point (the location of the spectral switch). However, the curvatures do play a role in influencing the rates of change for the relative spectral shifts and the positions of spectral switches. It can be seen that, for the $K < 0$ case, the relative spectral shift curve is stretched larger as the absolute value of K increases. This property indicates that the spectral shift is decelerated in the curved space with negative constant curvatures, resulting in the locations of occurring spectral switches farther away from the light source. In the $K > 0$ case, the curve of the relative spectral shift is shrunken, indicating the acceleration of the spectral shift in curved space with positive Gaussian curvatures and resulting in the locations of spectral switches closer to the source for larger values of K . With the increase of K , these curves are more and more shrunken.

Figure 5(b) shows the changes of the relative spectral shifts for different values of the spatial correlation length σ_0 . When the light sources are partially coherent, the magnitudes of the relative spectral shifts become smaller as the value of σ_0 decreases. Meanwhile, as the value of σ_0 decreases, the relative spectral shift curve smooths away the discontinuity point at the farthest position of the light source, and the amount of blueshift and redshift corresponding to other discontinuity points will also decrease. For example, the spectral switch happens near $z/z_0 = 0.26$ on the flat surface. Its blueshift has decreased from 0.167 to 0.123 and its redshift value has decreased from 0.193 to 0.171. Thus, as the source changes from fully coherent light to partially coherent light, the valley of the modifier becomes shallower, which may lead to the valley of the output spectrum also becoming shallower and disappearing. That may finally result in the disappearance of the spectral switch phenomenon.

In order to study the change of the fully coherent light source's spectral switch position with Gaussian curvature K

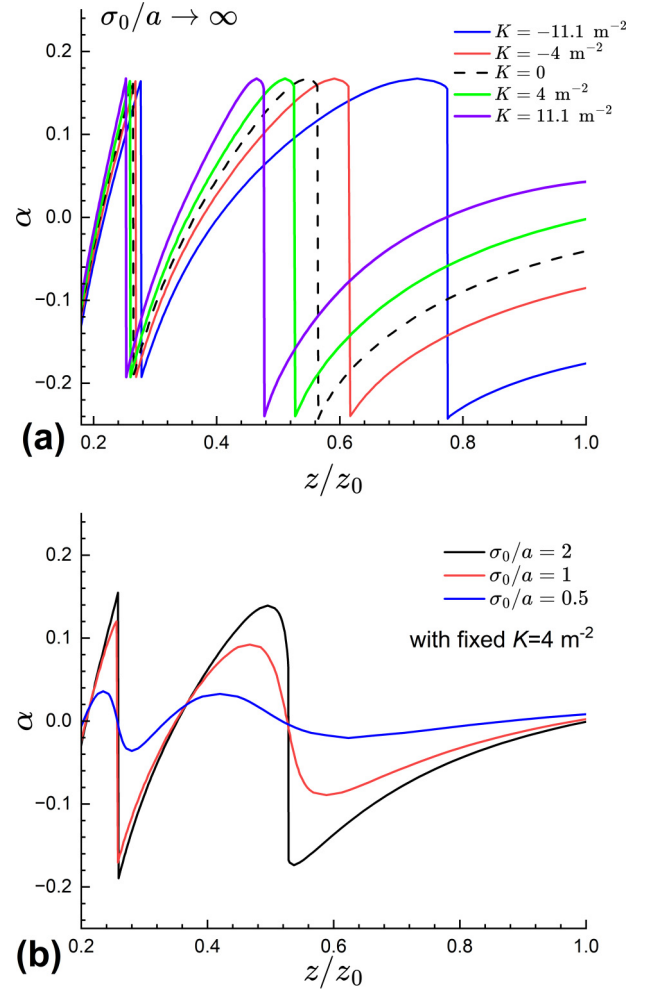


FIG. 5. Effects of (a) the curvatures of surfaces and (b) the spatial correlation of light on the behaviors of spectral switches. In (a) the light sources are fully coherent, i.e., $\sigma_0/a \rightarrow \infty$. In (b) the surface has the constant Gaussian curvature $K = 4 \text{ m}^{-2}$.

in more detail, we expand the range of $|K|$ to $[1, 200] \text{ m}^{-2}$ and select 21 different values of K , including ten negative K , ten positive K , and one null K . For each K , we calculate the precise positions of three different kinds of spectral switches. The results are shown in Fig. 6. It is worth mentioning that for positive curvature the range of z is $|z| < \pi R/2$ and for negative curvature its range becomes $|z| < R \sinh^{-1}(1)$ with $R = r_0$. Additionally, on surfaces with negative Gaussian curvature, as the value of $|K|$ increases, certain spectral switches may not occur due to the fact that the positions for occurrence of the corresponding order spectral switches are beyond the range of z ; hence the number of points of each spectral switch in Fig. 6 is actually smaller than 21.

Figure 6 shows that the curves are monotonically decreasing with the increase of K from negative to positive. This phenomenon can be explained by the decelerating and accelerating properties of the curved surfaces. The negative curvature decelerates the spectral shift, causing the relative spectral shift curve to be stretched, thereby increasing the distance of spectral switch positions away from the source. As K increases, the decelerate property is weakened. In contrast, the positive

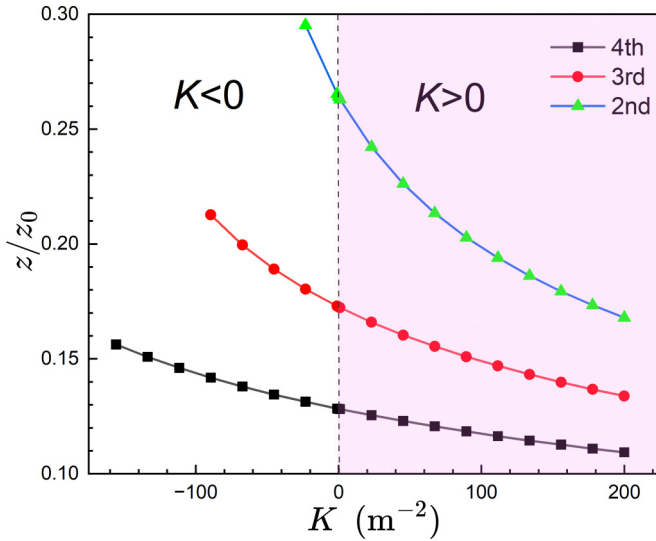


FIG. 6. Effect of space curvatures on positions of on-axis spectral switches. Here three kinds of spectral switches, corresponding, from top to bottom to the second-, third-, and fourth-order spectral switches, are demonstrated. The parameter $R = r_0$ is chosen.

curvature accelerates the spectral shift, resulting in the relative spectral shift curve being shrunken and the positions of spectral switches being closer to the source. As K increases, the acceleration property becomes more pronounced. Therefore, in the process of K changing from negative to positive, the spectral switches are first away from the source and then keep approaching the source. The curves in the second quadrant are shorter than those in the first quadrant. This is because some of the spectral switch points are stretched off the surface when $K < 0$.

By comparing the corresponding curves of different kinds of spectral switches, it can also be seen that the sensitivity of different spectral switches to K change is different. The overall slope of the curve corresponding to the second spectral switch is greater than that of the third spectral switch, and the overall slope of the third is greater than that of the fourth. Among these three types of spectral switches, the second spectral switch is the most sensitive, followed by the third and

the fourth. So the smaller the order of the spectral switch is, the more sensitive it is to the change of Gaussian curvature K .

IV. CONCLUSION

We have investigated the phenomenon of spectral switches in 2D curved space, which is described here by surfaces of revolution with constant Gaussian curvature. We have derived the expression of the output on-axis spectrum from a finite source with width $2a$ by using the paraxial approximation. By defining the effective propagation distance on curved surfaces, the theoretically approximate solution of the on-axis spectral switch was presented and the on-axis spectral switches were classified. Similar to flat space, spectral switches of fully coherent sources in curved space are also induced by diffraction. Nevertheless, the curvature of curved surfaces changes the effective propagation distance of light and thus leads to different effective Fresnel numbers in curved space. This theoretical method can provide sufficient precision for estimating the positions of spectral switches in curved space with constant Gaussian curvature.

Comparing the relative spectral shift curves for different K , we found that positive Gaussian curvature has a longitudinal compression effect on the relative spectral shift curve and the negative Gaussian curvature surface has a longitudinal stretching effect on the curve. This effect becomes more and more evident with the increase of K , but the jump magnitudes at these discontinuity points on the curves do not change compared with that in flat space. It also reveals the change of the positions of spectral switches with the change of K for the fully coherent light and shows the influence of the spatial coherence of light on the on-axis spectral change for the polychromatic partially coherent light source during propagation.

The effects of off-axis spectral switches and various surfaces of revolution are open to further exploration. These results on the spectral effects of light in curved space can promote an understanding of the change of light spectra in non-Euclidean space.

ACKNOWLEDGMENTS

This research was supported by the National Natural Science Foundation of China (Grants No. 62375241 and No. 11974309).

- [1] G. Rousseaux, C. Mathis, P. Maïssa, T. G. Philbin, and U. Leonhardt, Observation of negative-frequency waves in a water tank: A classical analogue to the Hawking effect? *New J. Phys.* **10**, 053015 (2008).
- [2] L.-P. Euvé, F. Michel, R. Parentani, T. G. Philbin, and G. Rousseaux, Observation of noise correlated by the Hawking effect in a water tank, *Phys. Rev. Lett.* **117**, 121301 (2016).
- [3] J. Steinhauer, Observation of quantum Hawking radiation and its entanglement in an analogue black hole, *Nat. Phys.* **12**, 959 (2016).
- [4] S. Eckel, A. Kumar, T. Jacobson, I. B. Spielman, and G. K. Campbell, A rapidly expanding Bose-Einstein condensate: An expanding universe in the lab, *Phys. Rev. X* **8**, 021021 (2018).
- [5] J. Drori, Y. Rosenberg, D. Bermudez, Y. Silberberg, and U. Leonhardt, Observation of stimulated Hawking radiation in an optical analogue, *Phys. Rev. Lett.* **122**, 010404 (2019).
- [6] H. S. Nguyen, D. Gerace, I. Carusotto, D. Sanvitto, E. Galopin, A. Lemaître, I. Sagnes, J. Bloch, and A. Amo, Acoustic black hole in a stationary hydrodynamic flow of microcavity polaritons, *Phys. Rev. Lett.* **114**, 036402 (2015).
- [7] D. Vocke, C. Maitland, A. Prain, K. E. Wilson, F. Biancalana, E. M. Wright, F. Marino, and D. Faccio, Rotating black hole geometries in a two-dimensional photon superfluid, *Optica* **5**, 1099 (2018).
- [8] C. Barceló, S. Liberati, and M. Visser, Analogue gravity, *Living Rev. Relativ.* **14**, 3 (2011).

- [9] C. Barceló, Analogue black-hole horizons, *Nat. Phys.* **15**, 210 (2019).
- [10] S. L. Braunstein, M. Faizal, L. M. Krauss, F. Marino, and N. A. Shah, Analogue simulations of quantum gravity with fluids, *Nat. Rev. Phys.* **5**, 612 (2023).
- [11] R. C. T. da Costa, Quantum mechanics of a constrained particle, *Phys. Rev. A* **23**, 1982 (1981).
- [12] S. Longhi, Topological optical Bloch oscillations in a deformed slab waveguide, *Opt. Lett.* **32**, 2647 (2007).
- [13] G. Della Valle, M. Savoini, M. Ornigotti, P. Laporta, V. Foglietti, M. Finazzi, L. Duò, and S. Longhi, Experimental observation of a photon bouncing ball, *Phys. Rev. Lett.* **102**, 180402 (2009).
- [14] A. Szameit, F. Dreisow, M. Heinrich, R. Keil, S. Nolte, A. Tünnermann, and S. Longhi, Geometric potential and transport in photonic topological crystals, *Phys. Rev. Lett.* **104**, 150403 (2010).
- [15] A. Libster-Hershko, R. Shiloh, and A. Arie, Surface plasmon polaritons on curved surfaces, *Optica* **6**, 115 (2019).
- [16] J. Bělič, T. Tyc, and S. A. R. Horsley, Optical simulation of quantum mechanics on the Möbius strip, Klein's bottle and other manifolds, and Talbot effect, *New J. Phys.* **23**, 033003 (2021).
- [17] S. Batz and U. Peschel, Linear and nonlinear optics in curved space, *Phys. Rev. A* **78**, 043821 (2008).
- [18] V. H. Schultheiss, S. Batz, A. Szameit, F. Dreisow, S. Nolte, A. Tünnermann, S. Longhi, and U. Peschel, Optics in curved space, *Phys. Rev. Lett.* **105**, 143901 (2010).
- [19] V. H. Schultheiss, S. Batz, and U. Peschel, Hanbury Brown and Twiss measurements in curved space, *Nat. Photonics* **10**, 106 (2016).
- [20] C. Xu, A. Abbas, L.-G. Wang, S.-Y. Zhu, and M. S. Zubairy, Wolf effect of partially coherent light fields in two-dimensional curved space, *Phys. Rev. A* **97**, 063827 (2018).
- [21] A. Patsyk, M. A. Bandres, R. Bekenstein, and M. Segev, Observation of accelerating wave packets in curved space, *Phys. Rev. X* **8**, 011001 (2018).
- [22] A. Patsyk, U. Sivan, M. Segev, and M. A. Bandres, Observation of branched flow of light, *Nature (London)* **583**, 60 (2020).
- [23] R. Bekenstein, Y. Kabessa, Y. Sharabi, O. Tal, N. Engheta, G. Eisenstein, A. J. Agranat, and M. Segev, Control of light by curved space in nanophotonic structures, *Nat. Photonics* **11**, 664 (2017).
- [24] C. Xu, A. Abbas, and L.-G. Wang, Generalization of Wolf effect of light on arbitrary two-dimensional surface of revolution, *Opt. Express* **26**, 33263 (2018).
- [25] C. Xu and L.-G. Wang, Theory of light propagation in arbitrary two-dimensional curved space, *Photonics Res.* **9**, 2486 (2021).
- [26] J. Zhang, C. Xu, P. Sebbah, and L.-G. Wang, Diffraction limit of light in curved space, *Photonics Res.* **12**, 235 (2024).
- [27] B. A. Garetz, Angular Doppler effect, *J. Opt. Soc. Am.* **71**, 609 (1981).
- [28] M. P. J. Lavery, F. C. Speirits, S. M. Barnett, and M. J. Padgett, Detection of a spinning object using light's orbital angular momentum, *Science* **341**, 537 (2013).
- [29] E. Wolf, Invariance of the spectrum of light on propagation, *Phys. Rev. Lett.* **56**, 1370 (1986).
- [30] E. Wolf, Non-cosmological redshifts of spectral lines, *Nature (London)* **326**, 363 (1987).
- [31] E. Wolf and D. F. V. James, Correlation-induced spectral changes, *Rep. Prog. Phys.* **59**, 771 (1996).
- [32] J.-J. Greffet, R. Carminati, K. Joulain, J.-P. Mulet, S. Mainguy, and Y. Chen, Coherent emission of light by thermal sources, *Nature (London)* **416**, 61 (2002).
- [33] G. M. Morris and D. Faklis, Effects of source correlation on the spectrum of light, *Opt. Commun.* **62**, 5 (1987).
- [34] M. F. Bocko, D. H. Douglass, and R. S. Knox, Observation of frequency shifts of spectral lines due to source correlations, *Phys. Rev. Lett.* **58**, 2649 (1987).
- [35] E. Wolf, T. Shirai, H. Chen, and W. Wanh, Coherence filters and their uses I. Basic theory and examples, *J. Mod. Opt.* **44**, 1345 (1997).
- [36] T. Shirai, E. Wolf, H. Chen, and W. Wang, Coherence filters and their uses II. One-dimensional realizations, *J. Mod. Opt.* **45**, 799 (1998).
- [37] J. Pu, H. Zhang, and S. Nemoto, Spectral shifts and spectral switches of partially coherent light passing through an aperture, *Opt. Commun.* **162**, 57 (1999).
- [38] J. T. Foley and E. Wolf, Phenomenon of spectral switches as a new effect in singular optics with polychromatic light, *J. Opt. Soc. Am. A* **19**, 2510 (2002).
- [39] J. Pu, S. Nemoto, and B. Lü, Effect of spectral correlations on spectral switches in the diffraction of partially coherent light, *J. Opt. Soc. Am. A* **20**, 1933 (2003).
- [40] H. C. Kandpal, Experimental observation of the phenomenon of spectral switch, *J. Opt. A* **3**, 296 (2001).
- [41] H. C. Kandpal, S. Anand, and J. S. Vaishya, Experimental observation of the phenomenon of spectral switching for a class of partially coherent light, *IEEE J. Quantum Electron.* **38**, 336 (2002).
- [42] S. Anand, B. K. Yadav, and H. C. Kandpal, Experimental study of the phenomenon of $1 \times N$ spectral switch due to diffraction of partially coherent light, *J. Opt. Soc. Am. A* **19**, 2223 (2002).
- [43] B. K. Yadav, S. A. M. Rizvi, and H. C. Kandpal, Experimental observation of spectral changes of partially coherent light in Young's experiment, *J. Opt. A* **8**, 72 (2006).
- [44] J. Li and L. Chang, Spectral shifts and spectral switches of light generated by scattering of arbitrary coherent waves from a quasi-homogeneous media, *Opt. Express* **23**, 16602 (2015).
- [45] X. Wang, Z. Liu, and K. Huang, Multiple spectral switches generated by the scattering of a novel electromagnetic random source of circular frame upon a semisoft boundary medium, *Laser Phys. Lett.* **16**, 066005 (2019).
- [46] Y. Zhang and J. Zhou, Spectral shifts and spectral switches of polychromatic stochastic electromagnetic vortex beams on scattering from a semisoft boundary medium, *J. Opt.* **21**, 045608 (2019).
- [47] P. Han, Near field lattice spectroscopy with a reflective confocal configuration, *Appl. Phys. Express* **4**, 022401 (2011).
- [48] J. Pu, C. Chi, and S. Nemoto, Spectral anomalies in Young's double-slit interference experiment, *Opt. Express* **12**, 5131 (2004).
- [49] P. Han, All optical spectral switches, *Opt. Lett.* **37**, 2319 (2012).
- [50] L. Mandel and E. Wolf, *Optical Coherence and Quantum Optics*, 1st ed. (Cambridge University Press, Cambridge, 1995).